Three-Dimensional p-Adaptive Computation of Electrostatic Force and Energy

Jian-She Wang and Nathan Ida, *Member, IEEE*

***Abstract*—This paper discusses a p-adaptive finite element method for electrostatic force and energy computation based on the constitutive error criterion, and the implementation on a three-dimensional mixed polyhedral grid. The method is applied to simple MEMS structures and the convergence characteristic is demonstrated.**

***Index Terms*—Adaptive meshing, electrostatics, finite element method, error analysis.**

I. Introduction

RECENT advances in Micro-Electro-Mechanical Systems (MEMS) [1] have triggered renewed interests in precision computation of electrostatic forces and energy. In spite of the fact that finite element analysis of electrostatic devices is a well-established field [2], such interests arise mostly from practical considerations. A Typical MEMS device involves high density and complex three-dimensional (3D) micro-geometry, and requires precision electrostatic force and capacitance prediction vs. geometrical motional locations. These considerations point at an *intelligent* self-adaptive 3D simulation tool that is capable of precision prediction, and yet at tractable computational cost. Such a simulation tool is precisely the aim of the present paper. Specifically the paper addresses the implementation of a p-adaptive finite element method (FEM) [3] up to 8th orders on a mixed polyhedral grid, and the associated error estimation criterion based on constitutive error [4]–[8].

II. Formulation and Constitutive Error

The computational 3D space domain Ω is shown in Fig. 1. The exterior boundary Γ_0 is assumed to be located in n homogeneous, isotropic dielectric medium with a dielectric constant ε. Inside Ω, there exist inhomogeneous media represented by a dielectric tensor $[\varepsilon]$. Across a pair of electrodes, Γ_1 and Γ_2, an electric voltage V_s is applied. The computational objective is to predict capacitance, and the force distribution on electrodes which may be movable.

The underlying electrostatic field is governed by Maxwell's equations in the absence of charge:

$$\nabla \times \mathbf{E} = 0, \tag{1}$$

$$\nabla \cdot \mathbf{D} = 0, \tag{2}$$

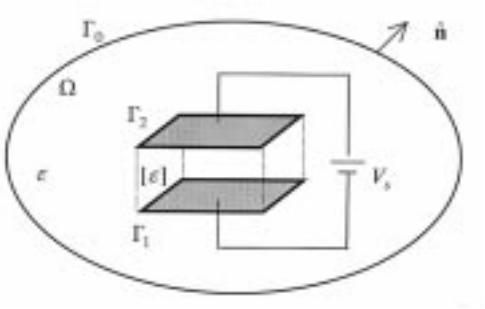

Fig. 1. Computational space domain under consideration.

along with a dielectric constitutive equation:

$$\mathbf{D} = [\varepsilon] \cdot \mathbf{E}, \tag{3}$$

subject to these boundary conditions:

$$\hat{\mathbf{n}} \times \mathbf{E}|_{\Gamma_e} = 0, \tag{4}$$

$$\hat{\mathbf{n}} \cdot \mathbf{D}|_{\Gamma_d} = 0, \tag{5}$$

where $\hat{\mathbf{n}}$ is the outward normal, and the domain outer boundary Γ_0 is decomposed into two parts, Γ_e and Γ_d.

The mathematical structure in (1)—(5) suggests two complementary systems [2]. In the E-system, the electric field strength $\mathbf{E}$ may be represented by the gradient of an electric potential (voltage):

$$\mathbf{E} = -\nabla V \tag{6}$$

which fulfills (1) and (4). A solution is obtained by solving (2). In the D-system, the electric displacement $\mathbf{D}$ may be represented by the curl of a vector potential:

$$\mathbf{D} = \nabla \times \mathbf{K} \tag{7}$$

which fulfills (2) and (5). A solution is then obtained by solving (1). If a solution $\mathbf{E}$ from the E-system, or a solution $\mathbf{D}$ from the D-system satisfies the constitutive equation (3), then the pair $(\mathbf{E}, \mathbf{D})$ would be the true solution of the problem considered. Or, there exists a constitutive error [4], [5]:

$$\mathbf{e} = \mathbf{D} - [\varepsilon] \cdot \mathbf{E}, \tag{8}$$

which should be minimized through an adaptive h- or p-refinement until a prescribed tolerance is reached. This dual process is mathematically rigorous except that computational cost is high

Manuscript received October 25, 1999.
J. S. Wang is with Ansys, Inc., Canonsburg, PA 15317 USA.
N. Ida is with The University of Akron, Akron, OH 44325 USA.
Publisher Item Identifier S 0018-9464(00)05638-7.

for practical devices, since two independent solutions have to be attempted before the error can be assessed.

The present approach, along with others [5]–[7], is to pursue first an FEM solution via the E-system:

$$\int_{\Omega} \nabla N_1 \cdot [\varepsilon] \cdot \nabla V \, d\Omega - \int_{\Gamma} N_s \hat{\mathbf{n}} \cdot \mathbf{D} \, d\Gamma = 0, \qquad (9)$$

where N_i denote FEM shape functions. The electrode voltage condition (internal to the domain as shown in Fig. 1):

$$V|_{\Gamma_2} - V|_{\Gamma_1} = 0 \qquad (10)$$

can be enforced when solving (9), in addition to the boundary conditions (4) and (5).

A second solution $\mathbf{D}$, satisfying the Maxwell's equations and boundary conditions, may be then constructed posteriori, thus relieving the computational burden of having to solve the problem twice. Instead of introducing a vector potential $\mathbf{K}$, a solution is sought in a finite element, of the form:

$$\hat{\mathbf{D}} = \sum_n d_n \mathbf{F}_n, \qquad (11)$$

where $\mathbf{F}_n$'s are normally continuous, *vector* functions [9] that belong to the functional space H(div). This specific choice helps automatically maintaining the boundary condition (5). There exist apparently many possibilities to construct (11). One rigorous approach is the 'traction recovery' procedure by Ladeveze [4] and implemented for magnetostatics in [6]. It is found that Ladeveze's procedure can be very complicated for 3D finite elements with higher p-levels, and therefore, an alternative approach involving simple averaging operation [7] is used to construct $\hat{\mathbf{D}}$. The averaging operation is performed on each element interface, excluding any infinitely thin electrode surface. On any interface with known surface charge, the surface jump condition must be incorporated also.

To measure the error (8), the energy norm over the whole domain is used:

$$||\mathbf{e}||_{\Omega} = \left[\int_{\Omega} \mathbf{e}^T \cdot [\varepsilon] \cdot \mathbf{e} \, d\Omega \right]^{1/2}. \qquad (12)$$

From the pair $(\mathbf{E}, \hat{\mathbf{D}})$, it is now possible to compute the relative constitutive error:

$$\varepsilon_{\Omega} = \frac{||\hat{\mathbf{D}} - [\varepsilon] \cdot \mathbf{E}||_{\Omega}}{||\hat{\mathbf{D}} + [\varepsilon] \cdot \mathbf{E}||_{\Omega}}, \qquad (12)$$

The global relative error (12) is seen as the sum of element contributions:

$$e_{\Omega}^2 = \sum_E e_E^2, \qquad (13)$$

where the relative error for an element E is given by:

$$e_E = \frac{||\hat{\mathbf{D}} - [\varepsilon] \cdot \mathbf{E}||_E}{||\hat{\mathbf{D}} + [\varepsilon] \cdot \mathbf{E}||_{\Omega}}. \qquad (14)$$

The global error (12) helps to quantify the quality of the approximate pair $(\mathbf{E}, \hat{\mathbf{D}})$, while the element error (14) allows to localize the error distribution in the solution domain as required for p-enrichment. The implementation of the procedure is explained next.

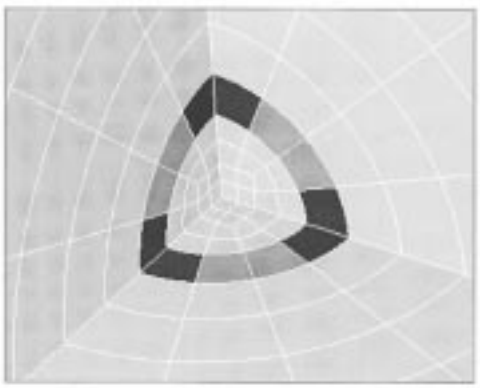

Fig. 2. Element p-levels for the charged sphere. Light: $p = 2$. Gray: $p = 4$. Dark: $p = 5$.

III. p-Refinement Strategy in Polyhedral Mesh

From a practical point of view, it is preferable to invoke error control based on energy, field, or force quantities. In the present implementation, the following adaptive strategy is employed:

i) Start with a finite element mesh with corner- and mid-nodes (i.e., $p = 2$)
ii) Obtain solution. Iterative equation solver is preferred
iii) Calculate global-wise energy, force, and/or point-wise electric field values. Up to ten such specifications may be requested
iv) Check convergence. Stop if tolerance is met
v) Exit if maximum p-level (= 8) is reached
vi) Compute element relative error distribution
vii) Raise p-level of elements with larger relative constitutive error and go to step ii)

Step v) is based on the consideration that convergence may not be reached if the starting mesh is too coarse. Under this case, a refined mesh should be generated, and the process may be tried again.

Modern finite element mesh generators are capable of generating finite element meshes consisting of hexahedral, tetrahedral, and prism (wedge) shapes. The inter-element geometrical compatibility is maintained by using standard second order functions, i.e., eight-noded mapping for a quadrilateral face and six node mapping for a triangular face. The hierarchical shape functions up to eighth order are decomposing into *nodal*, *edge*, *face* and *body* groups [3], [10]. This practice has the advantage of maintaining C^0 continuity for voltage during selective element p-enrichment. For example, an element with $p = 2$ may be interfaced with an element with $p = 4$ by simply eliminating face functions of $p = 3$ & 4 on the shared face.

IV. Validation and MEMS Application Example

To validate the present procedure and implementation, a simple test case is considered first, where the electric field of a uniformed charged sphere is computed and compared against analytical result. The geometrical mesh is shown in Fig. 2.

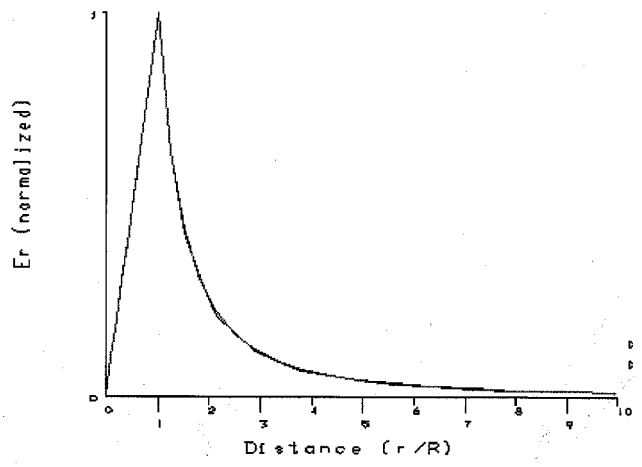

Fig. 3. The comparison of electric field values for the charged sphere. Solid line: numerical; dashed line: analytical.

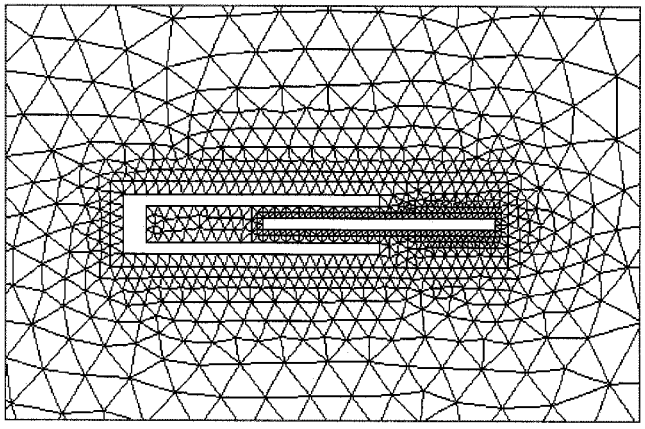

Fig. 4. The geometrical wedge mesh (2D view), all starting at $p = 2$.

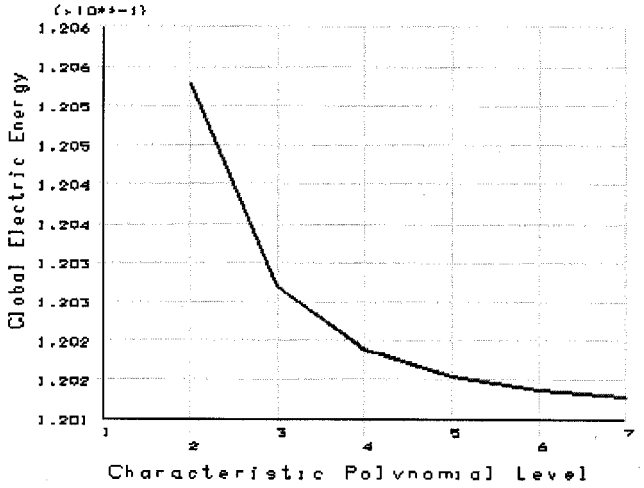

Fig. 5. Convergence characteristics of stored energy vs. highest p-level.

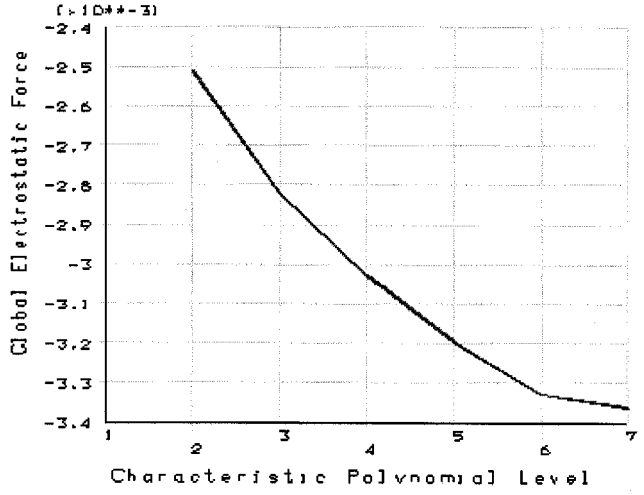

Fig. 6. Convergence characteristics of computed electrostatic force vs. highest p-level.

A tolerance of 0.5% of the radial electric field at the sphere radius between subsequent p-loops, is requested. The elements next to the sphere radius are raised to $p = 4$ or 5 by the adaptive solver as shown in Fig. 2. This is as expected, since the electric undergoes a transition form a linear variation within the sphere, to a $1/r^2$ variation outside the sphere. The final electric field vs. radial distance is shown Fig. 3, and the comparison with analytical values is found excellent.

Next, a simple electrostatic comb drive structure is detailed. The dimensions are taken from [11], and geometry along with the mesh may be seen in Fig. 4. The electric field of the structure is assumed two-dimensional but the problem is solved as a three-dimensional problem with one layer wedge mesh. The fingers have a width 2 μm, a length of 40 μm, and gap is 2 μm. The moving finger (beam) is grounded, and the fixed finger (U-shaped) is supplied with a voltage. The objective is to compute the electrostatic force per unit depth exerted on the moving finger. The Maxwell stress tensor method is used to compute force.

The mesh density is determined ad hoc, and by conventional wisdom it should produce a reasonably accurate force value even at $p = 2$. Also, a pretty large elliptical cylindrical boundary (not shown) is used to simulate the far field effect. Since the exact value of electrostatic force is not known, the intention here is to demonstrate how the force value would change as the element p-levels are enriched. The convergence characteristics of the computed global stored energy and electrostatic force vs. highest p-levels are shown in Figs. 5 and 6, respectively. Two observations can be made, assuming that there is a minimum value for energy and a maximum value for force as suggested by the curves. 1) The predicted (converged) force value is 30% higher that that by $p = 2$: our conventional wisdom of mesh being good enough could be wrong. 2) These curves suggest that the global stored energy is converging much faster than the force,. This is as expected, since the force computation accuracy depends on local field accuracy as well as on global accuracy, and thus is more computationally demanding.

One might wonder why the curve slope in Fig. 6 is not as steep as it may be desired. The reason lies in the fact that elements are selectively enriched, since a uniform p-enrichment for all elements is deemed costly, if not impossible. In fact, only a small percentage of elements are upgraded to higher p-levels,

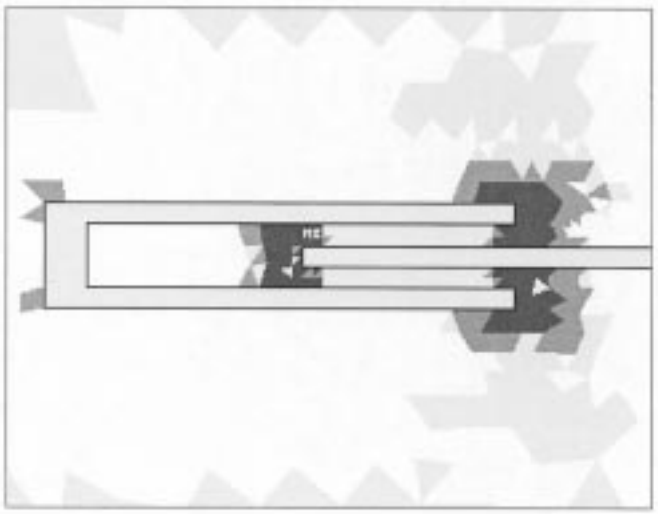

Fig. 7. Element p-level. Light gray: $p = 3$. Grey: $p = 4$ & 5. Dark gray: $p = 6$ & 7.

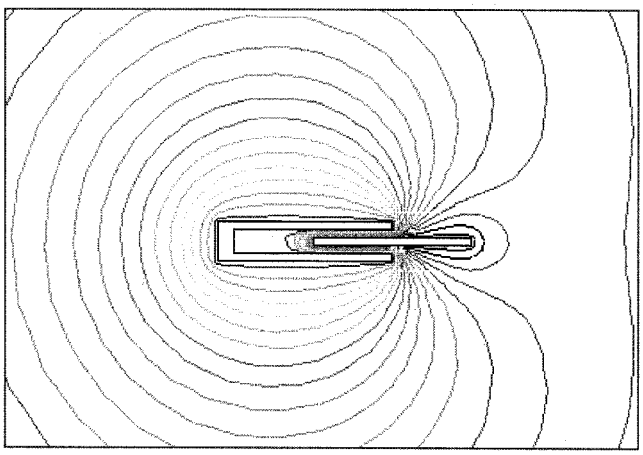

Fig. 8. The voltage contour plot for the 2D MEMS drive.

as demonstrated in Fig. 7. By comparing the upgraded element clustering with higher p-levels, with the voltage contour plot shown in Fig. 8, one can see that the present adaptive procedure is enriching elements in the critical regions such as the gap entrants, where field gradient is larger. Fig. 7 seems also to be suggesting that by increasing the geometrical mesh density, or starting with higher p-levels in the highlighted regions, a much faster solution may be achieved.

Three-dimensional version of the comb drive analysis was also carried out. The corresponding voltage contour plot is shown in Fig. 9. Convergence performance data similar to Figs. 5 and 6 have been obtained.

V. Summary

A 3D p-version finite element method has been implemented for adaptive computation of electrostatic force and energy

Fig. 9. The voltage contour plot for the 3D comb drive.

computation. For the demonstrated numerical examples in MEMS applications, the constitutive error approach, combined with a simple second field construction, has been found effective in locating critical regions for p-enrichment.

It is expected that the second field construction based on Ladeveze's traction recovery, should be more effective. The corresponding investigation is directed to future work.

References

[1] R. T. Howe, S. Muller, K. J. Gabriel, and W. S. N. Trimmer, "Silicon micromechanics: Sensors and actuators on a chip," *IEEE Spectrum*, pp. 29–35, July 1990.

[2] J. A. H. Rikabi, C. F. Bryant, and E. M. Freeman, "Complementary solutions of electrostatic field problems," *IEEE Trans. Magnetics*, vol. 25, no. 6, pp. 4427–4442, 1989.

[3] B. Szabo and I. Babuska, *Finite Element Analysis*, NY, Wiley 1991.

[4] P. Ladeveze, G. Goffignal, J. P. Pelle, and I. Babuska *et al.*, *Accuracy Estimates and Adaptive Refinements in Finite Element Computation*: John Wiley & Sons, 1986, pp. 181–203.

[5] N. A. Golias, T. D. Tsiboukis, and A. Bossavit, "Constitutive inconsistency: Rigorous solution of Maxwell's equations based on a dual approach," *IEEE Trans. Magnetics*, vol. 30, no. 5, pp. 3586–3589, 1984.

[6] J.-F. Remacle, P. Dular, F. Henrotte, A. Genon, and W. Lagros, "Error estimation and mesh optimization using error in constitutive relation for electromagnetic field computation," *IEEE Trans. Magnetics*, vol. 31, no. 6, pp. 3587–3589, 1995.

[7] J.-F. Remacle, C. Geuzaine, P. Dular, H. Hedia, and W. Lagros, "Error estimation based on a new principle of projection and reconstruction," *IEEE Trans. Magnetics*, vol. 34, no. 5, pp. 3264–3267, 1998.

[8] K. C. Chellamuthu and N. Ida, "Reliability assessment of an 'a posteriori' error estimate for adaptive computation of electromagnetic field problems," *IEEE Trans. Magnetics*, vol. 31, no. 3, pp. 1761–1764, 1995.

[9] J.-S. Wang and N. Ida, "Curvilinear and higher order 'edge' elements in electromagnetic field computation," *IEEE Trans. Magnetics*, vol. 29, no. 2, pp. 1491–4194, 1993.

[10] P. Carnevali, R. B. Morris, Y. Tsuji, and G. Taylor, "New basis functions and computational procedures for p-version finite element analysis," *Int. J. Numer. Meth. Engr.*, vol. 36, pp. 3759–3799, 1993.

[11] F. Shi, P. Ramesh, and S. Mukherjee, "Dynamic analysis of micro-electromechanical systems," *Int. J. Numer. Meth. Engr.*, vol. 39, pp. 4119–4139, 1996.